

## Understanding Surface Photochemistry from First Principles: The Case of CO-NiO(100)

Imed Mehdaoui\*

*Institut für Reine und Angewandte Chemie, Carl von Ossietzky Universität Oldenburg, Postfach 2503, D-26111 Oldenburg, Germany*

Thorsten Klüner†

*Institut für Reine und Angewandte Chemie, Carl von Ossietzky Universität Oldenburg, Postfach 2503, D-26111 Oldenburg, Germany*

(Received 28 September 2006; published 17 January 2007)

The excitation mechanism in the CO-NiO(100) system induced by a uv-laser pulse has been investigated from first principles. For the laser-driven process, the relevant electronically excited states are identified, and it is shown that a transition within the CO molecule is the crucial excitation step rather than substrate mediated processes. A new mechanism is proposed, in which the formation of a genuine C-Ni bond in the excited state is the driving force for photodesorption rather than electrostatic interactions, as has been found in similar systems. This results in very high velocities of CO molecules desorbing from the NiO(100) surface after electronic relaxation.

DOI: [10.1103/PhysRevLett.98.037601](https://doi.org/10.1103/PhysRevLett.98.037601)

PACS numbers: 79.20.La, 71.10.Li

A detailed mechanistic understanding of surface photochemistry is of fundamental interest in photocatalysis, quantum control of chemical reactions on surfaces, or solar energy conversion. For this reason, the study of photo-induced processes and excited state properties of adsorbate substrate systems is crucial for advancement in these research fields. Experimentally, the intrinsic complexity of this task can be reduced by considering the simplest photochemical reaction on surfaces, i.e., laser-induced desorption. Although a vast amount of experimental data for photodesorption processes of various adsorbate substrate systems has been obtained in the past decade, most experimental studies suffer from the lack of sufficient theoretical support due to the exceedingly difficult task of an accurate calculation of electronic excitations on surfaces. As a consequence, experimental data are sparsely understood concerning the atomistic mechanism of photodesorption. To our knowledge, only a few theoretical studies were pursued up to a level of sophistication which allows for a detailed understanding of experimental results, even containing a predictive character. In these studies, photodesorption of diatomic molecules such as CO, NO, and O<sub>2</sub> from substrates such as NiO(100), Cr<sub>2</sub>O<sub>3</sub>(0001), and TiO<sub>2</sub>(110) have been investigated using quantum chemical embedded cluster calculations and wave packet simulations [1–5]. In fact, electrostatic interactions were found to be the driving force for all systems under investigation, either due to a charge transfer between adsorbate and substrate [NO-NiO(100) [1]; O<sub>2</sub>-TiO<sub>2</sub> [5]] or due to the interaction of electric multipole moments with the field gradient above the ionic surface [CO-Cr<sub>2</sub>O<sub>3</sub>(0001) [2]]. This is in contrast to the CO-NiO(100) system investigated here, where the formation of a genuine C-Ni bond turns out to be the driving force for the dynamics of CO molecules on the NiO(100) surface.

In the laser-induced desorption experiment, an epitaxially grown film of NiO(100) on Ni(100) has been used.

Since the bonding of CO to NiO(100) is very local (for a detailed discussion, see, for example, Ref. [6]), a Ni<sub>5</sub>Mg<sub>13</sub><sup>18+</sup> cluster embedded in a field of 2906 point charges (PCF) has been used as an approximation for the NiO(100) film. The geometry of the cluster model corresponds to the ideal rocksalt structure of bulk NiO with a lattice constant of 4.176 Å [7] (see Fig. 1). All complete active space self-consistent field (CASSCF) and second-order complete active space perturbation theory (CASPT2) calculations were performed using the MOLCAS package of programs [8]. Details on the basis set used for the quantum chemical calculations can be found in Ref. [9].

Using this model, the geometry of the CO-Ni<sub>5</sub>Mg<sub>13</sub><sup>18+</sup> adsorbate substrate complex was optimized at the CASPT2 level, keeping the cluster coordinates frozen. The active space of the CASSCF calculations included the 3d<sub>z<sup>2</sup></sub> and

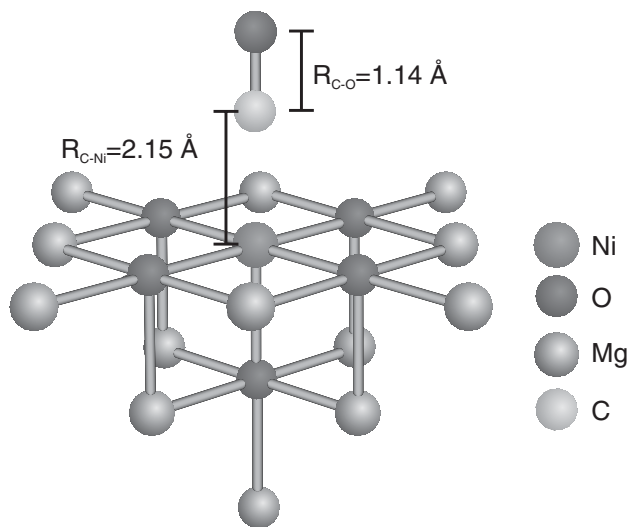


FIG. 1. Minimum energy geometry of CO on the Ni<sub>5</sub>Mg<sub>13</sub><sup>18+</sup> cluster in the ground state. The point charge field used is not shown.

$3d_{x^2-y^2}$  orbitals of the Ni atom and two active electrons in high spin configuration. In the CASPT2 calculations, the Ni  $1s$ ,  $2sp$ , and  $3sp$ , the Mg  $1s$  and  $2sp$ , the O  $1s$ , and the C  $1s$  orbitals were excluded from the correlation space.

In the minimum energy geometry, the CO molecule is located atop the central Ni atom (see Fig. 1). The CO axis is parallel to the surface normal with a C-O bond length of 1.14 Å, in good agreement with the experimentally measured value of 1.15 Å [10]. The C-Ni distance is 2.15 Å, which slightly overestimates the experimental finding of 2.07 Å [10] by 0.08 Å, indicating a somewhat weaker C-Ni bond strength than experimentally observed.

The adsorption energy was then calculated at the CASSCF and CASPT2 level. The results are summarized in Table I. At the CASSCF level, the CO-cluster interaction, which is almost entirely electrostatic in nature with very small covalent bonding contributions [11], is clearly repulsive (0.29 eV), where the BSSE (basis set superposition error) has been corrected by the counterpoise approach as proposed by Boys and Bernardi [12]. The corresponding adsorption energy at the CASPT2 level is  $-0.10$  eV, underestimating the experimental observation of  $-0.30$  eV [13] by 0.20 eV. These results are in good agreement with a recent study of Pacchioni *et al.* [6], in which the adsorption energy has been studied using both the CASPT2 method and density functional theory (DFT). In this study, Pacchioni *et al.* pointed out that the DFT results of a cluster model compared to periodic slab calculations give virtually the same adsorption energy with a difference of only 0.02 eV, which led to the conclusion that a cluster model properly describes the NiO(100) surface concerning local bonding effects. Thus, we pursue a local cluster approach for a reliable calculation of excited states as well.

Redlich *et al.* proposed a transition within the CO adsorbate, which corresponds to a  $5\sigma \rightarrow 2\pi^*(a^3\Pi)$  transition in the CO molecule in gas phase, as the crucial excitation step in laser-induced desorption [14]. This is in contrast to the NO-NiO(100) system, where a charge transfer state, resulting in an  $\text{NO}^-$ -NiO $^+$  species, is the decisive excited state [1] in similar photoinduced desorption experiments [15,16]. To verify whether a  $5\sigma \rightarrow 2\pi^*(a^3\Pi)$ -like transition is of important relevance, initially the excitation energies of gas phase CO in the ground state  $X^1\Sigma^+$  to the  $A^1\Pi$  and  $a^3\Pi$  excited states were calculated using the CASSCF and CASPT2 methods with two different active spaces (see Table II) to estimate the accuracy of these methods for this system. In the CASPT2 calculations, the  $1s$  and  $2s$  orbitals of O and C were not correlated. The bond

TABLE I. Adsorption energy of CO on the NiO<sub>5</sub>Mg<sub>13</sub><sup>18+</sup>/PCF cluster; in parentheses are values without BSSE correction.

Method	Adsorption energy (eV)
CASSCF(2, 2)	0.29 (0.21)
CASPT2	$-0.10$ ( $-0.40$ )
Experiment	$-0.30$

length of  $R_{\text{CO}} = 1.128$  Å corresponds to the experimental value for gas phase CO.

The CASSCF(10, 8) calculations included all valence electrons and orbitals of the CO molecule in the active space, whereas in the CASSCF(2, 3) the size of the active space was reduced, now containing only the  $5\sigma$  and the  $2\pi^*$  antibonding orbitals and two active electrons. Using the CAS(10, 8) active space, the excitation energy at the CASPT2 level from the ground state to the  $A^1\Pi$  state, which is the lowest dipole-allowed electronic transition, is 8.38 eV. This is in good agreement with experiment (8.51 eV). The excitation energy to the  $a^3\Pi$  state, which is the lowest electronically excited state, is 6.03 eV, also in good agreement with the experimental finding of 6.32 eV [17].

The CAS(2, 3) active space yields an excitation energy at the CASPT2 level to the  $A^1\Pi$  state of 8.22 eV, whereas the excitation energy to the  $a^3\Pi$  state yields 6.02 eV. Although a minimal active space has been used in these calculations, the experimental excitation energies are underestimated by only 0.29 and 0.30 eV. This result has importance for the CO-cluster calculations, since only a limited set of active orbitals can be used due to the size of the system.

The corresponding values at the CASSCF level show discrepancies up to 1.1 eV and, therefore, are not accurate in predicting correct excitation energies for CO molecules in gas phase.

To elucidate if a  $5\sigma \rightarrow 2\pi^*$ -like excitation within the CO-NiO(100) adsorbate substrate complex is in the range of the laser pulse energy of 4.66 eV used in the experiment, several excited states were calculated at the CASPT2 level for the CO-NiO<sub>5</sub>Mg<sub>13</sub><sup>18+</sup>/PCF system. The active space in the CASSCF calculations included the  $3d_{z^2}$  and  $3d_{x^2-y^2}$  orbitals of the Ni atom and the  $5\sigma$  and the two  $2\pi^*$  antibonding orbitals of the C atom and 4 active electrons. For consistency, also the  $\tilde{X}^3B_1$  ground state was calculated using the same active space. In the CASPT2 calculations, the Ni  $1s$ ,  $2sp$ , and  $3sp$ , the Mg  $1s$  and  $2sp$ , the O  $1s$ , and the C  $1s$  orbitals were not correlated.

Table III illustrates that the excitation energy to the  $\tilde{a}^5E$  state is 6.18 eV at the CASPT2 level, similar to the  $X^1\Sigma^+ \rightarrow a^3\Pi$  excitation energy for gas phase CO (see Table II), which points out that the CO-cluster interaction is very weak in this case.

TABLE II. Vertical excitation energies relative to ground state  $X^1\Sigma^+$  CO ( $R_e = 1.128$  Å).

State	Excitation energy (eV)				Experiment <sup>a</sup>
	CAS(10, 8)		CAS(2, 3)		
	CASSCF	CASPT2	CASSCF	CASPT2	
$A^1\Pi$	9.62	8.38	9.52	8.22	8.51
$a^3\Pi$	6.97	6.03	6.36	6.02	6.32

<sup>a</sup>Reference [17].

TABLE III. Vertical excitation energies on CASPT2 level from a CAS(4,5) reference relative to ground state  $\tilde{X}^3B_1$  CO-NiO<sub>5</sub>Mg<sub>13</sub><sup>18+</sup>/PCF.

State	Excitation energy (eV) CASPT2
$\tilde{a}^5E$	6.18
$\tilde{A}^3E$	4.54
$\tilde{a}^1E$	4.34

The vertical excitation energies to the  $\tilde{a}^1E$  and  $\tilde{A}^3E$  states are 4.34 and 4.54 eV at the CASPT2 level, respectively. Taking into account that the corresponding values for gas phase CO underestimate the experimental findings by about 0.3 eV, these results are in excellent agreement with the laser pulse energy of 4.66 eV used in the experiment, indicating that these excited states are of particular importance in the CO-cluster excitation.

Figure 2 illustrates the active natural molecular orbitals (MOs) of the  $\tilde{A}^3E$  state for the CO-NiO<sub>5</sub>Mg<sub>13</sub><sup>18+</sup>/PCF system in the minimum energy geometry of the ground state. The MOs of the  $\tilde{a}^1E$  and  $\tilde{a}^5E$  state differ only in the occupation numbers of the natural orbitals and are therefore not shown. The top left MO consists basically of a positive linear combination of the  $5\sigma$  orbital of the CO molecule and the  $3d_{z^2}$  orbital of the Ni atom, with an orbital occupation number of 1.51. The MO at the top middle represents the corresponding negative linear combination of these orbitals with an orbital occupation number of 0.49. The MOs at the top right and the bottom represent the  $3d_{x^2-y^2}$  and  $2\pi^*$  orbitals of the Ni atom and CO molecule with orbital occupation numbers of 1.0 and 0.5, respectively. Because of spin pairing, a covalent C-Ni

bond is formed, which leads to an orbital occupation number of 1.51 in the first MO. Consequently, the energy of the system is reduced compared to the  $\tilde{a}^5E$  state, resulting in a decrease in the excitation energy by about 1.6–4.54 eV.

In order to provide an insight into the dynamics of the desorption process, the potential energy curves of all relevant states were calculated and are illustrated in Fig. 3. The surface distance  $Z$  represents the distance between the center of mass of the CO molecule and the surface of the NiO<sub>5</sub>Mg<sub>13</sub><sup>18+</sup> cluster. The C-O bond length was kept fixed at  $R_{CO} = 1.143$  Å. The  $\tilde{a}^5E$  state is clearly repulsive due to the nonexistent spin pairing in the  $5\sigma - 3d_{z^2}$ -like MO. Because of the fixed CO bond length, the excitation energy of 5.81 eV in the asymptotic region is decreased compared to gas phase CO. In contrast to the  $\tilde{a}^5E$  and the ground state, which is almost entirely electrostatic in nature, the  $\tilde{a}^1E$  and  $\tilde{A}^3E$  excited states show pronounced attractive potential energy curves with a bond strength of about 2.1 eV, due to the formation of a covalent C-Ni bond. The large gradient at the Franck-Condon point of these potential energy curves suggests an Antoniewicz-like [18] mechanism for the laser-induced dynamics of the CO molecules. According to this scenario, the CO molecules will accelerate towards the NiO(100) surface upon laser excitation. After relaxation to the repulsive region of the ground state, the CO molecules will gain further kinetic energy and desorb with high velocities as observed experimentally. Thus, the formation of a genuine chemical bond turns out to be the driving force of photodesorption in the CO-NiO(100) system.

From a mechanistic point of view, this desorption scenario is qualitatively different from the NO-NiO(100), O<sub>2</sub>-TiO<sub>2</sub>, and CO-Cr<sub>2</sub>O<sub>3</sub> systems, which have been treated

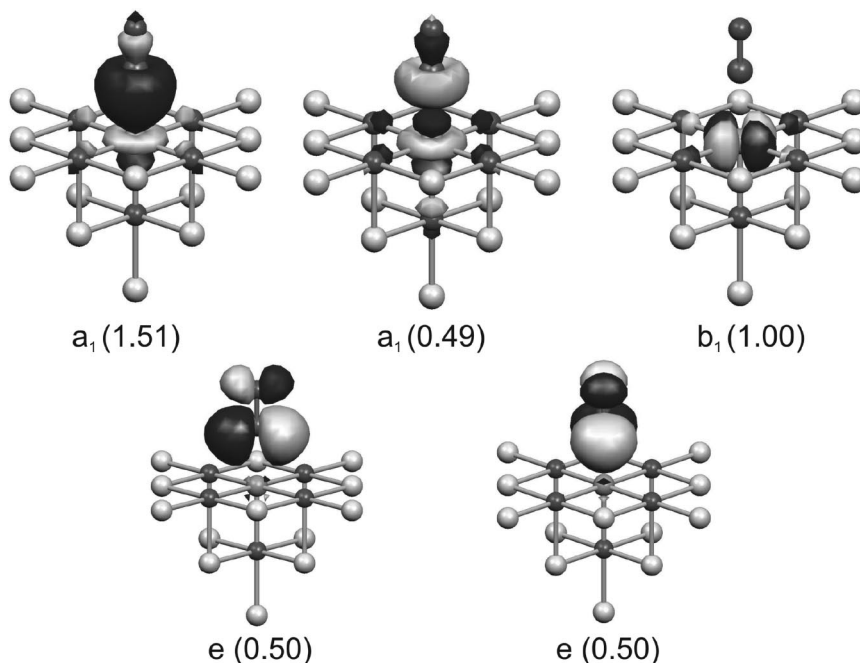


FIG. 2. Active natural molecular orbitals of CO-NiO<sub>5</sub>Mg<sub>13</sub><sup>18+</sup>/PCF from CASSCF(4,5) of the  $\tilde{A}^3E$  excited state. The geometry corresponds to the adsorption minimum of the ground state; occupation numbers of the natural orbitals are in parentheses. Illustrations were obtained using the MOLEKEL program [21,22].

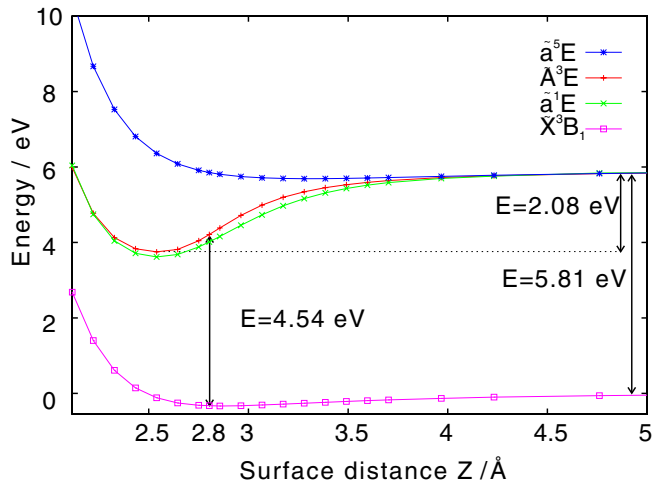


FIG. 3 (color online). Potential energy curves along the desorption coordinate  $Z$  for the ground state  $\tilde{X}^3B_1$  (squares) and the excited states  $\tilde{a}^5E$  (asterisks),  $\tilde{A}^3E$  (plus signs), and  $\tilde{a}^1E$  (crosses) of CO-NiO<sub>5</sub>Mg<sub>13</sub><sup>18+</sup>/PCF computed at the CASPT2 level. The C-O distance has been kept fixed to  $R_{CO} = 1.143$  Å. The curves have not been corrected for the BSSE.

on a similar level of sophistication [1,2,5,9,19,20]. In the NO-NiO(100) and O<sub>2</sub>-TiO<sub>2</sub> systems, charge transfer states are of prime importance in the photoinduced desorption processes. In particular, in the NO-NiO(100) system a charge transfer from the surface to the adsorbate results in a predominantly electrostatic interaction upon laser excitation. This results in an anti-Antoniewicz mechanism, where the NO molecules initially depart from the surface, then reach a turning point due to Coulomb attraction and eventually accelerate towards the surface [9,19]. Interestingly, electrostatic forces also dominate the mechanism of photoinduced desorption in the CO-Cr<sub>2</sub>O<sub>3</sub> system, where, similar to the CO-NiO(100) system in the present study, a  $5\sigma \rightarrow 2\pi^*$ -like excitation turns out to be the relevant excitation step. However, the electrostatic interaction of the electric quadrupole moment with the electric field gradient of the polar surface is the driving force in this photodesorption scenario [2].

In conclusion, the excitation mechanism in laser-induced desorption of CO from NiO(100) has been investigated from first principles. The relevant electronically excited states are identified, and it has been shown that a transition within the CO molecule is the crucial excitation step in this system rather than substrate mediated processes, as found in many other systems. We have found that the formation of a genuine covalent chemical C-Ni bond in the relevant excited states is of particular importance to explain the unique experimental features such as high desorption velocities of the CO molecules. This is in contrast to similar systems such as NO-NiO(100), O<sub>2</sub>-TiO<sub>2</sub>, and CO-Cr<sub>2</sub>O<sub>3</sub>, in which electrostatic forces are the dominant interactions. Thus, for the first time the

formation of a genuine covalent chemical bond in the electronically excited state turns out to be the driving force in laser-induced desorption. Future quantum dynamical wave packet simulations will reveal further microscopic insight into the photodesorption scenario in the CO-NiO(100) system, which will pave the way for an atomistic quantum control of photochemistry at the nanoscale.

\*Also at Fritz-Haber-Institut der Max-Planck-Gesellschaft, Faradayweg 4-6, D-14195 Berlin, Germany.

†Corresponding author.

Electronic address: Thorsten.Kluener@uni-oldenburg.de

- [1] T. Klüner, H.-J. Freund, J. Freitag, and V. Staemmler, *J. Chem. Phys.* **104**, 10 030 (1996).
- [2] M. Pykavy, S. Thiel, and T. Klüner, *J. Phys. Chem. B* **106**, 12 556 (2002).
- [3] T. Klüner, H.-J. Freund, V. Staemmler, and R. Kosloff, *Phys. Rev. Lett.* **80**, 5208 (1998).
- [4] S. Borowski, T. Klüner, and H.-J. Freund, *J. Chem. Phys.* **119**, 10 367 (2003).
- [5] M. P. de Lara-Castells and J. L. Krause, *J. Chem. Phys.* **118**, 5098 (2003).
- [6] G. Pacchioni, C. D. Valentin, D. Dominguez-Ariza, F. Illas, T. Bredow, T. Klüner, and V. Staemmler, *J. Phys. Condens. Matter* **16**, S2497 (2004).
- [7] R. Newman and R. M. Chrenko, *Phys. Rev.* **114**, 1507 (1959).
- [8] G. Karlström *et al.*, *Comput. Mater. Sci.* **28**, 222 (2003).
- [9] I. Mehdaoui, D. Kröner, M. Pykavy, H.-J. Freund, and T. Klüner, *Phys. Chem. Chem. Phys.* **8**, 1584 (2006).
- [10] J. T. Hoelt, M. Kittel, M. Polcik, S. Bao, R. L. Toomes, J. H. Kang, D. P. Woodruff, M. Pascal, and C. L. A. Lamont, *Phys. Rev. Lett.* **87**, 086101 (2001).
- [11] G. Pacchioni and G. Cogliandro, *Surf. Sci.* **255**, 344 (1991).
- [12] S. F. Boys and F. Bernardi, *Mol. Phys.* **19**, 553 (1970).
- [13] R. Wichtendahl, M. Rodriguez-Rodrigo, U. Härtel, H. Kühlenbeck, and H.-J. Freund, *Surf. Sci.* **423**, 90 (1999).
- [14] B. Redlich, A. Kirilyuk, T. Hoger, G. Helden, G. Meijer, and H. Zacharias, *Chem. Phys. Lett.* **420**, 110 (2006).
- [15] T. Mull, B. Baumeister, M. Menges, H.-J. Freund, D. Weide, C. Fischer, and P. Andresen, *J. Chem. Phys.* **96**, 7108 (1992).
- [16] G. Eichhorn, M. Richter, K. Al-Shamery, and H. Zacharias, *J. Chem. Phys.* **111**, 386 (1999).
- [17] E. S. Nielsen, P. Jørgensen, and J. Odderhede, *J. Chem. Phys.* **73**, 6238 (1980).
- [18] P. R. Antoniewicz, *Phys. Rev. B* **21**, 3811 (1980).
- [19] D. Kröner, I. Mehdaoui, H.-J. Freund, and T. Klüner, *Chem. Phys. Lett.* **415**, 150 (2005).
- [20] S. Thiel, M. Pykavy, T. Klüner, H.-J. Freund, R. Kosloff, and V. Staemmler, *J. Chem. Phys.* **116**, 762 (2002).
- [21] MOLEKEL 4.3, P. Flükiger, H. P. Lüthi, S. Portmann, and J. Weber, Swiss Center for Scientific Computing, Manno, Switzerland, 2000–2002.
- [22] S. Portmann and H. P. Lüthi, *Chimia* **54**, 766 (2000).